Petrology and geochemistry of Proterozoic olivine tholeiite intrusives from the Central Crystallines of the western Arunachal Himalaya, India: evidence for a depleted mantle

Rajesh K. Srivastava*, Hari B. Srivastava and Vaibhava Srivastava

Department of Geology, Banaras Hindu University, Varanasi 221 005, India

A number of plugs and dykes of mafic rocks are encountered between Se La and Jung areas of the Central Crystalline rocks of western Arunanchal Himalaya. These mafic intrusives are emplaced within the Paleoproterozoic high to medium grade schists and gneisses of Se La Group. These mafic rocks are metamorphosed and composed of hornblende (~70%) and plagioclase showing granoblastic texture. Geochemically they show olivine tholeiitic characteristics. Appreciable amount of normative hypersthene and olivine is present in all samples. The geochemistry of high-field strength (+ rare-earth) elements suggests that these mafic rocks are co-genetic and derived from olivine tholeiite melt generated from a depleted lherzolite mantle source. These mafic rocks show very close geochemical similarities with mafic rocks reported from the western Himalaya. The satellite imageries suggest that these mafic intrusive rocks are exposed at intersection of major lineaments. The association of these mafic rocks with major lineaments, mostly fault planes, advocates that these originally deep seated intrusions have been upthrown and exposed along the fault planes.

Keywords: Arunachal Himalaya, depleted mantle, geochemistry, Kameng, mafic rocks, olivine tholeiite, Proterozoic.

EASTERN parts of the Himalaya – particularly western Arunachal Himalaya, i.e. West Kameng region and Tawang – are geologically least studied in comparison to other parts of the Himalaya. Although the Geological Survey of India has done geological mapping work, very little published work is available[1–4]. Most of these work present geological framework of the western Arunachal Himalaya with little information about the mafic magmatic rocks[5]. Limited petrological and geochemical data on mafic rocks from the Higher Himalayan Central Crystallines is available. Only few occurrences of depleted mantle derived mafic magmatic rocks emplaced within the Higher Himalayan Central Crystallines are reported from Vaikrita[6] and Bhagirathi–Yamuna valleys[7,8] of the western Himalaya. Thus, detailed study on such rocks in a Precambrian terrain may play an important role in understanding crustal evolution. In this communication, we report new occurrences of Proterozoic olivine tholeiitic mafic intrusive rocks emplaced within the Palaeoproterozoic Se La Group Central Crystallines and present preliminary results on their field-setting, petrology and geochemistry.

The study area lies north of the Main Central Thrust (MCT) and forms a part of Higher Himalayan Metamorphic Belt (Figure 1 *b*). Rocks of the area represent the Central Crystallines in the western Arunachal Himalaya where they have been designated as Se La Group[3,4] of early Palaeoproterozoic age. The Se La Group in the study area is represented by high-grade schists and gneisses of the Galensiniak Formation and metasediments including graphite-bearing schists of the Taliha Formation[4]. During the present investigation, many mafic intrusive rocks were observed from the Central Crystalline rocks, particularly exposed between Se La and Jung areas (Figure 1). These mafic rocks mainly occur as small plugs (~10–20 m radius). Few small dykes (~100–200 m in length and 2–5 m in width) are also encountered. These

*For correspondence. (e-mail: rajeshgeolbhu@yahoo.com)

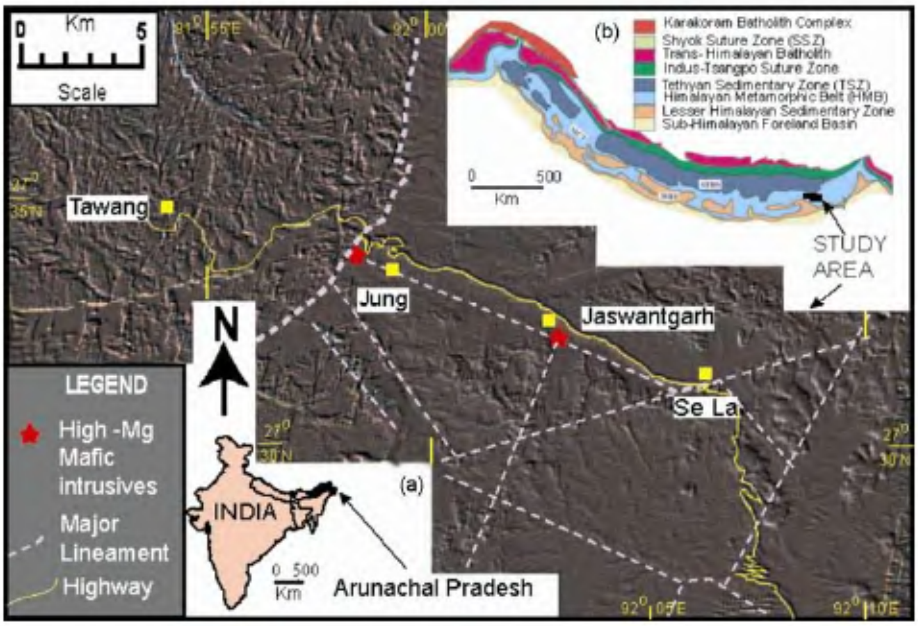

Figure 1. Mosaic of digitally processed satellite image highlighting the major lineaments. Locations of mafic intrusives are also depicted. Inset (a) shows map of India with location of Arunachal Pradesh and inset (b) shows location of the study area in the generalized geological map of Himalaya.

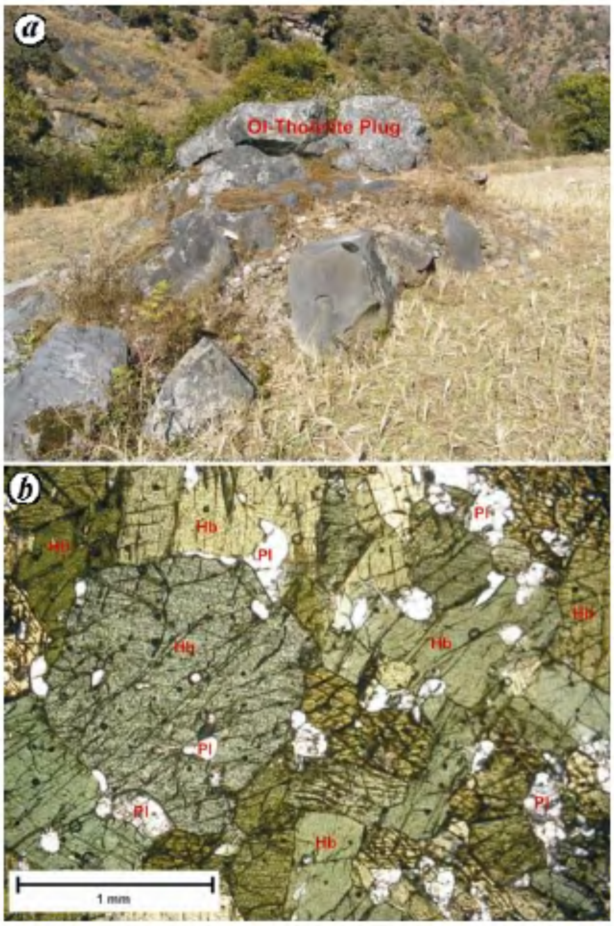

Figure 2. ***a***, A plug of olivine tholeiite mafic rock intrudes granite gneiss encountered near Jung. ***b***, Photomicrograph of studied rock. Hornblende grains are dominating over plagioclase feldspars.

mafic rocks intrude high to medium grade schists and gneisses. Best exposures of mafic intrusive rocks are encountered from Jung (Figure 2 *a*; as a plug) and Jaswantgarh. It is interesting to observe that these mafic bodies are exposed at the intersection of major lineaments, recognized on the satellite images (see Figure 1). The field relation of these intrusions suggests that they are exposed along fault zones. It therefore provides sufficient reason to believe that these intrusive rocks which were emplaced at a deeper level have come up and got exposed at the present level because of faulting.

All the studied mafic samples were examined for their petrographic characteristics. As these are metamorphosed, it is difficult to observe any igneous mineralogy. They are coarse-grained and show granoblastic texture and mainly consist of hornblende and plagioclase (Figure 2 *b*). Most of the samples are hornblende dominating (~70%). Plagioclase feldspars are present but not more than 25%. Hornblende grains are subhedral in shape and show poikiloblastic textures, defined by inclusions of plagioclase feldspars. Smaller grains are unsieved but larger hornblende grains are sieved with plagioclase feldspars. Two sets of oblique cleavages are observed in a number of hornblende grains. Plagioclase feldspar grains are untwined and smaller in size. Ilmenite and titanite are common minor constituents. Mineralogy of these rocks suggests their derivation from mafic protolith. Observed mineral assemblage suggests that studied mafic rocks are metamorphosed under medium grade metamorphic conditions.

Eleven samples were selected for this study for their whole rock major, trace and rare-earth element analyses.

Table 1. Whole rock major oxides (wt%) and CIPW norms of the olivine–tholeiite mafic rocks from the western Arunachal Himalaya

	32	33	41	42	44	47	51	56	75	76	85
Major oxides (wt%)											
SiO_2	46.48	46.67	45.71	45.66	46.81	45.18	47.05	43.86	45.63	46.85	46.82
TiO_2	1.17	1.24	1.19	1.00	0.98	1.00	0.85	0.84	1.05	1.12	1.02
Al_2O_3	16.63	16.32	15.89	15.09	14.49	14.80	16.81	12.41	16.26	16.78	17.14
Fe_2O_3	12.95	13.20	13.37	14.76	10.66	12.96	11.64	13.83	13.08	12.48	12.57
MnO	0.21	0.21	0.22	0.23	0.20	0.22	0.22	0.25	0.22	0.22	0.22
MgO	8.63	7.89	9.25	9.74	12.05	11.74	9.27	16.52	9.69	8.49	8.96
CaO	10.04	10.75	11.12	11.16	10.92	10.33	9.27	8.18	9.84	11.08	10.74
Na_2O	2.42	2.42	2.06	1.45	1.68	1.71	1.75	1.18	2.38	2.50	2.22
K_2O	0.97	0.19	0.20	0.27	0.56	0.29	1.98	0.21	0.30	0.27	0.31
P_2O_5	0.06	0.08	0.08	0.03	0.09	0.07	0.07	0.06	0.06	0.08	0.07
LOI	1.23	0.86	0.84	0.93	1.83	1.01	1.67	2.75	1.39	0.98	0.77
Total	100.80	99.82	99.92	100.30	100.30	99.31	100.60	100.10	99.90	100.90	100.80
Mg#	60.90	58.29	61.79	60.67	72.54	67.92	66.06	72.87	63.39	61.39	62.49
CIPW norm											
Or	5.69	1.14	1.19	1.60	3.32	1.74	12.21	1.26	1.81	1.63	1.89
Ab	17.52	20.79	17.59	12.30	14.26	14.74	15.45	10.19	20.52	21.59	19.39
An	37.89	35.38	36.94	38.36	36.30	35.07	27.56	33.85	34.48	35.05	32.12
Ne	1.51	–	–	–	–	–	–	–	–	–	–
Di	9.08	14.96	14.87	13.88	14.07	13.53	16.25	5.77	11.31	19.23	19.10
Hy	–	6.28	3.31	10.88	6.23	6.41	6.25	11.79	1.78	2.37	8.82
Ol	23.14	15.90	20.64	17.73	20.99	23.49	17.73	32.94	23.99	17.93	14.64
Mt	2.84	2.96	2.98	3.27	2.36	2.92	2.69	2.43	2.95	2.82	2.87
Il	2.20	2.39	2.28	1.90	1.87	1.93	1.68	1.63	2.03	2.17	2.00
Ap	0.14	0.19	0.19	0.07	0.21	0.16	0.17	0.14	0.14	0.19	0.17
Rock types (TAS Class[n])*	Alkali basalt	Sub-alkali basalt	Sub-alkali basalt	Sub-alkali basalt	Picrite	Sub-alkali basalt	Sub-alkali basalt	Picrite	Sub-alkali basalt	Sub-alkali basalt	Sub-alkali basalt

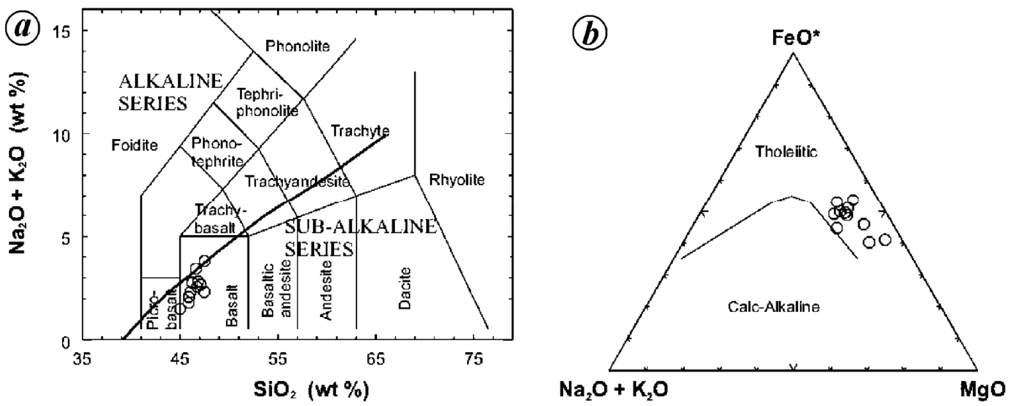

Figure 3. ***a***, Total-alkali and silica (TAS) diagram[9]. Thick line divides sub-alkaline basalts from alkaline basalts[10]. ***b***, AFM diagram[10].

The analyses were done at the Activation Laboratories Ltd., Ancaster, Ontario, Canada. ICP-OES (Model: Thermo-JarretAsh ENVIRO II) was used to analyse major elements, whereas ICP-MS (Model: Perkin Elmer Sciex ELAN 6000) was used to determine trace element concentrations. The precision is approximately 5% for major oxides and 5–10% for trace elements, when reported at 100× detection limit. Several standards, such as MRG1, W2, DNC1, STM1 and SY3 were run to check accuracy and precision. Major oxides and CIPW norms are presented in Table 1; Table 2 presents trace and rare-earth element compositions.

All the analysed mafic samples have moderate silica and high magnesium (~8 wt% or more) concentration. On the total-alkali and silica (TAS) classificatory diagram[9] (Figure 3 *a*) all samples show basaltic nature and fall

Table 2. Trace and rare-earth element (in ppm) compositions of the olivine tholeiite mafic rocks from the western Arunachal Himalaya

	32	33	41	42	44	47	51	56	75	76	85
Trace elements (ppm)											
Cr	260	180	230	240	590	430	280	700	320	240	190
Ba	36	37	12	22	9	8	94	5	86	37	24
Sr	158	173	167	87	96	105	132	132	177	206	146
Rb	51	7	4	7	23	6	266	2	10	4	8
Nb	2	3	3	2	2	2	5	2	2	2	2
Ta	0.2	0.2	0.2	0.2	0.2	0.2	0.3	0.1	0.2	0.2	0.2
Zr	28	41	36	39	66	38	37	26	34	33	30
Hf	1.1	1.3	1.4	1.2	1.9	1.0	1.3	0.9	1.0	1.1	1.1
Y	20	22	20	18	22	18	26	15	17	20	19
Th	0.4	0.6	0.6	0.8	2.2	0.5	1.1	0.4	0.5	0.5	0.5
U	0.2	0.2	0.1	0.1	0.4	0.1	0.6	3.6	0.1	0.1	0.1
Rare-earth elements (ppm)											
La	2.90	3.70	3.90	3.20	5.40	2.90	3.40	2.40	2.90	3.30	3.90
Ce	7.20	9.30	9.70	7.90	12.90	7.10	8.10	5.90	7.10	8.10	8.60
Pr	1.05	1.33	1.37	1.11	1.67	1.01	1.14	0.82	0.98	1.13	1.14
Nd	5.60	6.60	6.90	5.60	8.10	5.10	6.10	4.40	5.10	5.80	5.50
Sm	1.90	2.10	2.10	1.80	2.50	1.60	1.90	1.40	1.60	1.90	1.70
Eu	0.90	0.98	1.01	0.86	0.99	0.81	0.87	0.65	0.86	0.93	0.98
Gd	2.60	3.00	3.00	2.50	3.30	2.30	2.90	2.10	2.30	2.80	2.50
Tb	0.50	0.60	0.60	0.50	0.60	0.50	0.60	0.40	0.50	0.60	0.50
Dy	3.60	4.10	4.10	3.50	4.10	3.30	4.40	2.90	3.20	4.00	3.40
Ho	0.80	0.90	0.90	0.70	0.80	0.70	0.90	0.60	0.60	0.80	0.70
Er	2.40	2.70	2.60	2.20	2.50	2.20	2.90	1.90	2.00	2.40	2.20
Tm	0.37	0.41	0.40	0.34	0.37	0.33	0.48	0.30	0.30	0.37	0.33
Yb	2.40	2.70	2.60	2.20	2.40	2.20	3.10	2.00	2.00	2.40	2.20
Lu	0.37	0.41	0.40	0.34	0.36	0.34	0.48	0.30	0.31	0.39	0.33
Nb/Y	0.10	0.14	0.15	0.11	0.09	0.11	0.19	0.13	0.12	0.1	0.11

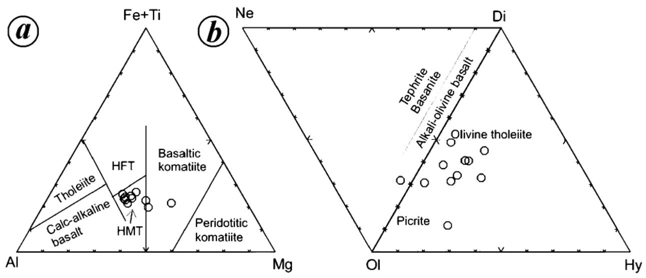

Figure 4. *a*, Jensen's cation diagram[11]. ***b***, Normative Di–Ol–Hy and Ol–Di–Ne triangular classificatory diagram[13].

towards picro-basalt field. This suggests their high-Mg nature. Figure 3 *a* also classifies studied rocks as sub-alkaline type[10]. AFM[10] (alkali, ferric and magnesium) compositions suggest tholeiitic nature of these rocks (Figure 3 *b*). Jensen cation plot[11] (Figure 4 *a*) is also used to classify these mafic rocks. This plot is useful to classify high-Mg rocks. Studied samples fall in the high-Mg tholeiitic (HMT) and basaltic komatiitic fields. This clearly suggests high-Mg nature of these rocks. High-Mg nature is also supported by moderate to high Mg-number of these rocks (Mg# varies between 58 and 73). CIPW norm of all the samples has been calculated with the latest computer program[12], which also uses TAS classification. This calculation classifies the mafic rocks for the present study into sub-alkaline basalt and picrite, as observed on the TAS diagram (Figure 3 *a*). Except one sample (No. 32), which has nepheline, all others have hypersthene and olivine besides diopside and opaques normative compositions. Normative albite is also present in appreciable amount. This composition suggests high-Mg nature of the studied rocks. Normative compositions are also plotted on Thompson's classificatory diagram[13] (Figure 4 *b*). This diagram corroborates high-Mg nature of studied rocks as they show olivine tholeiite, picrite and alkali-olivine basalt compositions. Thus, on the basis of geochemical and CIPW norm compositions and classificatory diagrams presented, studied mafic intrusive rocks may be classified as high-Mg tholeiitic mafic intrusive rocks.

A geochemical variation diagram of MgO vs SiO_2, TiO_2 and few high-field strength trace elements (HFSE) of the studied mafic rocks is used to evaluate crystallization behaviour (Figure 5). As studied rocks are altered due to medium grade metamorphism, mostly elements, such as Ti, Nb, Zr, Y and Nd, which are supposed to be immobile during such alterations are used[14] for this exercise. Good crystallization trends are observed in all the

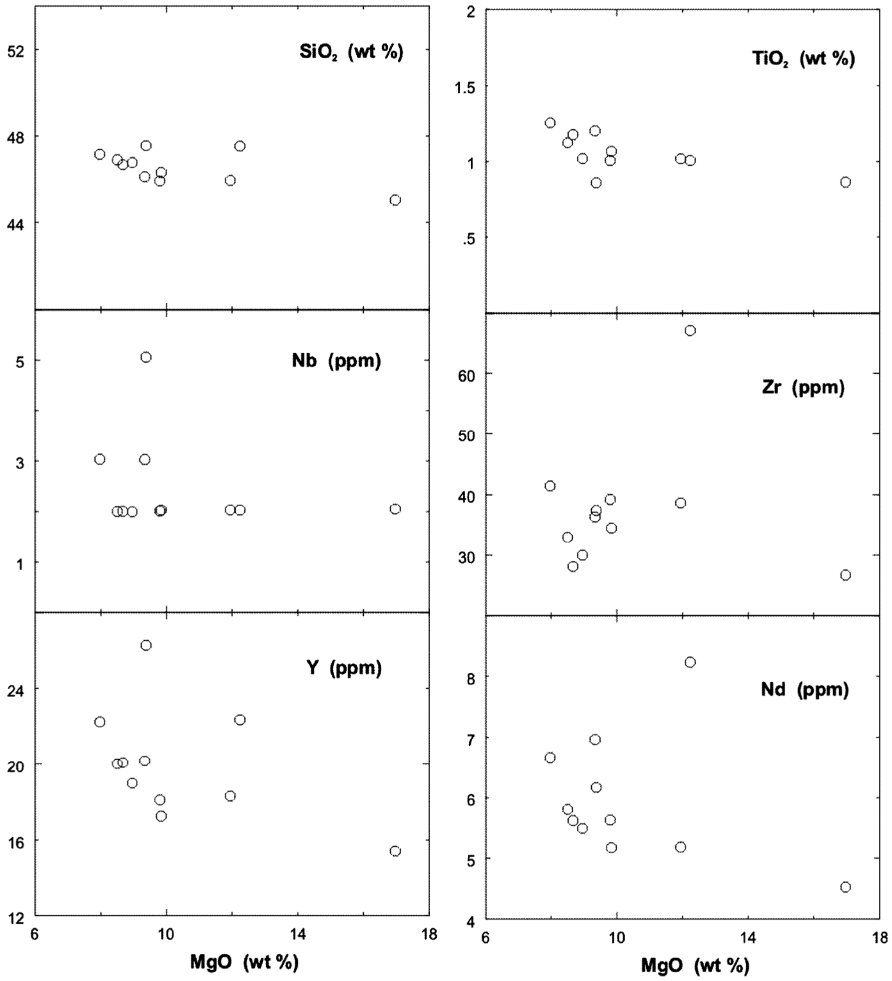

Figure 5. MgO variation diagrams.

plots. All the plotted elements including silica increase with decreasing MgO, suggesting normal crystallization behaviour. This also suggests co-genetic relationship between the studied samples. Observed MgO and SiO_2 correlation suggests fractionation of olivine during the course of crystallization of melt. Similar correlation with other plotted HFSEs suggests crystallization of accessory phases like sphene, zircon and ilmenite.

For further evaluation of geochemical characteristics, primordial mantle normalized multi-element spidergrams are also presented (Figure 6 *a*). Except Ba, all other plotted elements show more enriched compositions than the primordial mantle. Ba in one sample (No. 56) shows more depleted concentration than mantle. Large ion lithophile elements (LILE: Rb, Ba, Th and K) show wide range; probably because of alteration of studied mafic rocks by medium grade metamorphism. On the other hand, high-field strength elements (HFSE: Ta, Nb, La, Ce, Sr, Nd, Hf, Zr, Sm, Ti, Tb and Y) show very narrow and systematic range; this is because these elements are immobile during the alterations[14]. Ta and Nb anomalies are not very significant. Chondrite normalized rare-earth elements (REE) are presented in Figure 6 *b*. REEs show enriched compositions compared to the chondritic values. Parallel but flat REE patterns are observed. Light REE (LREE) show nominally lower concentration than heavy REE (HREE). Very small positive Eu anomaly is observed on REE patterns. This is probably because of plagioclase accumulation during the later stages of crystallization. This is also supported by small positive Sr anomaly on multi-element spidergrams (see Figure 6 *a*).

From the observed geochemical characteristics of the studied mafic intrusive rocks, the following inferences may be drawn.

1. Absence or small negative Nb and Ta anomalies on multi-element spidergrams, absence of enriched LREE patterns and presence of very consistent HFSE and REE patterns clearly do not suggest any significant role of crustal contamination.
2. These rocks are probably derived from a high-Mg (olivine rich) magma.

3. HREE concentrations of 10× chondrite suggest that melt responsible for the genesis of studied rocks is generated from a mantle with no garnet.
4. Flat overall REE patterns or small lower concentrations of LREE than HREE patterns, as observed in the present case, probably suggest their derivation from a primitive mantle source[15].

Thus, it is clear from the above presentation that studied mafic rocks are crystallized from an olivine tholeiite melt originated from a depleted mantle. Such melts (olivine tholeiite) may be generated from ~20% to 25% melting of a depleted mantle lherzolite source at about 15–20 kbar (ref. 16). Normative olivine compositions of studied rocks (between 15% and 34%; see Table 1) also support this inference.

The studied mafic magmatic rocks of Se La Group with two other similar occurrences from the western Himalayan Range[5–8], are compared for their geochemical characters. Strikingly similar multi-element and REE patterns were observed. On the multi-element spidergrams all the three occurrences show HFSE concentrations between 1× and 10× more than the primordial mantle compositions. They also exhibit either nil or insignificant Nb anomaly and small positive Sr anomaly. More interestingly REE patterns are very similar (Figure 7). This observation suggests that all these occurrences of mafic magmatic rocks reported from the Central Crystalline rocks have similar petrogenetic history. Ahmad *et al.*[6] suggested that mafic rocks from the Vaikrita Central Crystallines are derived from a depleted asthenospheric mantle and are unrelated to other mafic rocks of the region. It is also suggested that these distinct geochemical characteristics may be used to demarcate the Main Central Thrust along the Vaikrita Thrust[6]. Srivastava and Sahai[8] suggested the same for the mafic magmatic rocks reported from the Central Crystallines of the Bhagirath–Yamuna valleys. They inferred that these mafic rocks show closed geochemical similarities with the N-MORB and derived from a melt derived from a depleted mantle source. This interesting petrological and geochemical correlation of similar mafic magmatic rocks reported from different parts of Himalaya suggests existence of large mafic magmatic events during the Proterozoic. This distinct mafic magmatism probably played an important role in crustal evolution of the Higher Himalaya. More detailed field, petrological and geochemical study (including isotope geochemistry) together with age determination data is needed for any further discussion.

The petrological and geochemical characteristics of the mafic intrusive rocks from the central crystallines of the western Arunachal Himalaya lead to the following conclusions.

1. These rocks are exposed at the intersection of well recognized major lineaments between Se La and Jung areas within the Palaeoproterozoic high to medium grade schists and gneisses of Se La Group. The lineaments appear to be deep faults which have brought the mafic intrusions to the present level.

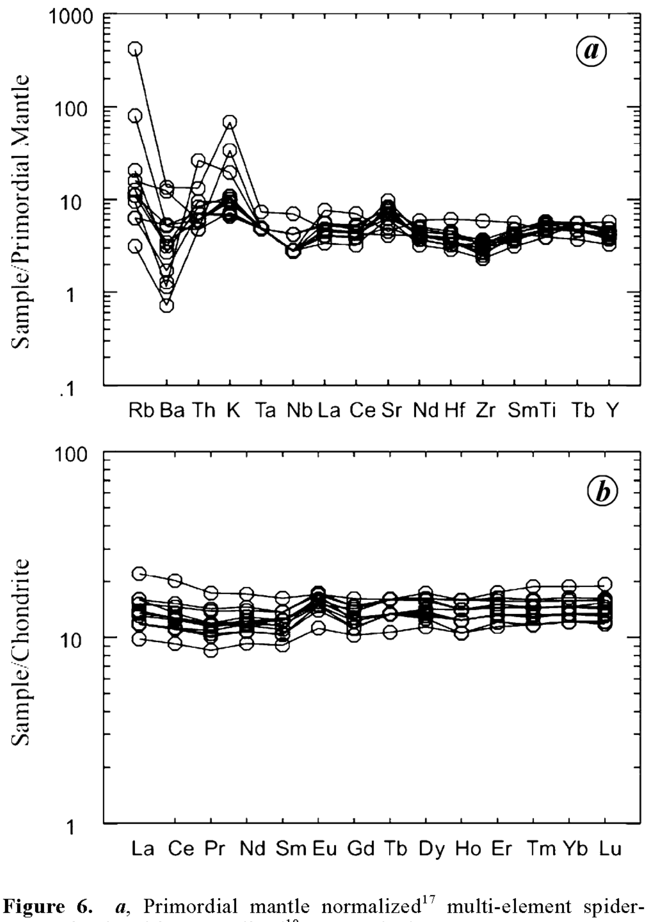

Figure 6. ***a***, Primordial mantle normalized[17] multi-element spidergrams. ***b***, Chondrite normalized[18] rare-earth element patterns.

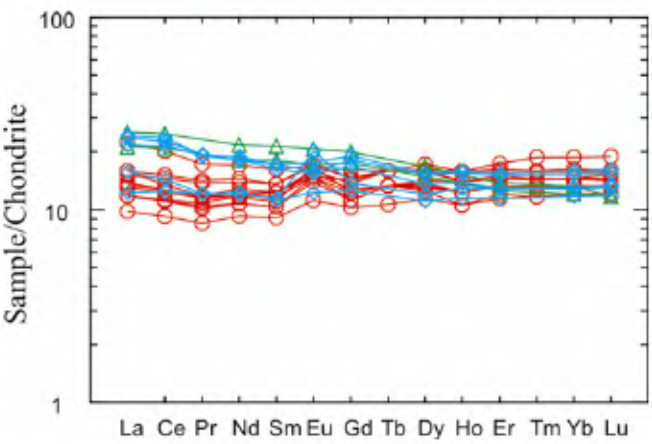

Figure 7. Comparison of rare-earth element patterns of mafic magmatic rocks from Higher Himalaya Central Crystallines. Symbols: open red circles – Se La mafic rocks (present study); open green triangles – Vaikrita mafic rocks[6]; open blue diamonds–Bhagirathi–Yamuna Valleys mafic rocks[8].

2. All these rocks are metamorphosed and show granoblastic texture. Hornblendes constitute more major proportions than plagioclase feldspar. Mineralogical composition suggests medium amphibolite grade metamorphic conditions.
3. Chemistry classifies these rocks as olivine tholeiitic mafic rocks. They contain appreciable amount of hypersthene and olivine in their normative compositions.
4. Trace elements particularly HFSE and REE compositions, suggest that all these rocks are co-genetic and probably derived from olivine tholeiite magma originated from a depleted mantle lherzolite source.
5. These mafic rocks show very close geochemical similarities with mafic rocks reported from the Central Crystallines of Western Himalaya, suggesting large mafic magmatic events during the Proterozoic.
6. These are preliminary results; more detailed work is required for the proper evaluation and establishment of a petrogenetic model for these interesting rocks.

1. Acharyya, S. K., Ghosh, S. C. and Ghosh, R. N., Geological framework of the eastern Himalayas in parts of Kameng, Subansari and Siang districts, Arunachal Pradesh. *Geol. Surv. India Misc. Publ.*, 1983, **43**, 145–152.
2. Bhushan, S. K., Bindal, C. M. and Aggarwal, R. K., Geology of Bomdila group in Arunachal Pradesh. *J. Himalayan Geol.*, 1991, **2**, 207–214.
3. Kumar, G., *Geology of Arunachal Pradesh*, Geological Society India, Bangalore, 1997, p. 217.
4. Bhattacharjee, S. and Nandy, S., Geology of the western Arunachal Himalaya in parts of Tawang and West Kameng districts, Arunachal Pradesh. *J. Geol. Soc. India*, 2007, **72**, 199–207.
5. Ahmad, T., Precambrian mafic magmatism in the Himalayan Mountain Range. *J. Geol. Soc. India*, 2008, **72**, 85–92.
6. Ahmad, T., Mukherjee, P. K. and Trivedi, J. R., Geochemistry of Precambrian mafic magmatic rocks of the Western Himalaya, India: petrogenetic and tectonic implications. *Chem. Geol.*, 1999, **160**, 103–119.
7. Sahai, A. and Srivastava, R. K., Structural and geochemical characteristics of amphibolites from the Bhagirathi and Yamuna valleys of Main Central Thrust Zone, Garhwal Himalaya. *Himalayan Geol.*, 1997, **18**, 191–201.
8. Srivastava, R. K. and Sahai, A., High-field strength element geochemistry of mafic intrusive rocks from the Bhagirathi and Yamuna valleys, Garhwal Himalaya, India. *Gondwana Res.*, 2001, **4**, 455–463.
9. Le Maitre, R. W., *Igneous Rocks: A Classification and Glossary of Terms*, Cambridge University Press, Cambridge, 2002, 2nd edn, p. 236.
10. Irvin, T. N. and Baragar, W. R. A., A guide to the chemical classification of the common volcanic rocks. *Can. J. Earth Sci.*, 1971, **8**, 523–548.
11. Jensen, L. S., *A New Cation Plot for Classifying Sub-alkaline Volcanic Rocks*, Ontario Div. Mines Misc. Paper No. 66, 1976.
12. Verma, S. P., Torres-Alvarado, I. S. and Sotelo-Rodríguez, Z. T., SINCLAS: standard igneous norm and volcanic rock classification system. *Computers Geosci.*, 2002, **28**, 711–715.
13. Thompson, R. N., Dispatches from the basalt front: 1. experiments. *Proc. Geol. Assoc. UK*, 1984, **95**, 249–262.
14. Rollinson, H., *Using Geochemical Data: Evolution, Presentation, Interpretation*, Longman Scientific and Technical, UK, 1993, p. 344.
15. Cullers, R. L. and Graf, J. L., Rare-earth elements in igneous rocks of the continental crust: predominantly basic and ultrabasic rocks. In *Rare Earth Element Geochemistry* (ed. Henderson, P.), Elsevier, Amsterdam, pp. 237–274.
16. Jaques, A. L. and Green, D. H., Anhydrous melting of oeridotite at 0–15 kb pressure and the genesis of tholeiitic basalts. *Contrib. Mineral. Petrol.*, 1980, **73**, 287–310.
17. McDonough, W. F., Sun, S.-S., Ringwood, A. E., Jagoutz, E. and Hofmann, A. W., K, Rb and Cs in the earth and moon and the evolution of the earth's mantle. *Geochim. Cosmochim. Acta*, 1992, **56**, 1001–1012.
18. Evensen, N. M., Hamilton, P. J. and O'Nion, R. K., Rare earth abundances in chondritic meteorites. *Geochim. Cosmochim. Acta*, 1978, **42**, 1199–1212.

ACKNOWLEDGEMENTS. We thank the Department of Science and Technology, New Delhi for financial assistance. We also thank N. V. Chalapathi Rao for his constructive comments on the previous version of this manuscript.

Received 9 March 2009; accepted 9 September 2009